LWT - Food Science and Technology 129 (2020) 109555

Contents lists available at ScienceDirect

LWT - Food Science and Technology

journal homepage: www.elsevier.com/locate/lwt

Pore characteristics and structural properties of ethanol-treated starch in relation to water absorption capacity

Achmat Sarifudin[a,d], Thewika Keeratiburana[e], Siriwat Soontaranon[b], Chaiyot Tangsathitkulchai[c], Sunanta Tongta[a,*]

[a] School of Food Technology, Institute of Agricultural Technology, Suranaree University of Technology, Muang, Nakhon Ratchasima, 30000, Thailand
[b] Synchrotron Light Research Institute (Public Organization), Muang, Nakhon Ratchasima, 30000, Thailand
[c] School of Chemical Engineering, Institute of Engineering, Suranaree University of Technology, Muang, Nakhon Ratchasima, 30000, Thailand
[d] Research Center for Appropriate Technology, Indonesian Institute of Sciences (P2TTG-LIPI), Jl. K.S. Tubun No. 5, Subang 41213, West Java, Indonesia
[e] Department of Food Science, Faculty of Science, Buriram Rajabhat University, Buriram, 31000, Thailand

ARTICLE INFO

Keywords:
Amorphous and V-Type crystalline structures
Ethanol-treated starch
Pore characteristics
Water absorption capacity

ABSTRACT

Ethanol-treated starch (ETS) is known to absorb a high amount of water at room temperature. The influences of pore characteristics and structural properties of ETS prepared from 4 different starch sources (maize, potato, cassava, and rice starches) at three conversion temperatures (80, 90 and 100 °C) on water absorption capacity (WAC) were investigated. The results indicate that ETS from maize and potato starches contain non-rigid and slit-shaped pores. For ETS from maize and potato starches, water penetrated the granules through the fissures, hydrated the amorphous regions, melted the V-type crystalline structure, and was held within the ETS granules upon water absorption. For non-granular ETS from cassava and rice starches, water hydrated the amorphous and V-type crystalline structures, and was entrapped within a three-dimensional network of starch components upon contact with water.

1. Introduction

Developing porous foods have recently become one of the most interesting research topics. New porous foods for specific applications, such as extruded products (Karathanos & Saravacos, 1993), encapsulating agents for flavor compounds (Weirong & Huiyuan, 2002), drug carriers (Najafi, Baghaie, & Ashori, 2016), and nutraceutical carriers (Wang et al., 2016) are increasingly in demand.

Pore characteristics are a fundamental property of porous materials that influence their macroscopic properties, such as bulk density, mechanical strength, and thermal conductivity (Sing et al., 1985). Investigation of these properties is necessary particularly for food industry since they are essential to choose suitable porous materials for specific applications, such as for adsorbents, catalysts, encapsulating agents, and pigment carriers (Lowell, Shields, Thomas, & Thommes, 2010). Materials with high porosity mostly possess a high surface area and pore diameter size within the micropore range (i.e., less than 2 nm) (Lowell et al., 2010; Sing et al., 1985).

Native starch granules are known to have low porosity. Nevertheless, they contain some sources of porosity within their granules. Hall and Sayre (1970) reported that wheat, rye, and barley starches exhibit surface pores. Moreover, Fannon, Hauber, and Bemiller (1992) stated that rice, oat, potato, tapioca, arrowroot, and canna starches do not have surface pores. However, the latest investigation suggests that all native starch granules contain pores of different sizes when the nitrogen sorption isotherm method is used to probe the porosity of starch granule (Sujka & Jamroz, 2010). The second source of porosity in native starch granules is their internal channels. Huber and BeMiller (1997) reported that they appear to be serpentine and they connect internal cavities or channels with openings on the surface of the granules. The pore size of native starch granules has been characterized such as most native starches have pores with a diameter of about 2–3 nm, while pores of native corn and rice starches have a diameter of 100–200 nm (Lesław Juszczak, Fortuna, & Wodnicka, 2002; Sujka & Jamroz, 2010); however, the other pore characteristics of native starch granules such as pore rigidity properties have not yet been reported.

Water absorption capacity is one method that can be used to evaluate the porosity of starch granules (Wang et al., 2016). Water molecules penetrate the inner region of a starch granule via the granule

* Corresponding author.
E-mail addresses: achmat.sarifudin@lipi.go.id (A. Sarifudin), thewika.kt@bru.ac.th (T. Keeratiburana), siriwat@slri.or.th (S. Soontaranon), chaiyot@sut.ac.th (C. Tangsathitkulchai), s-tongta@g.sut.ac.th (S. Tongta).

https://doi.org/10.1016/j.lwt.2020.109555
Received 22 November 2019; Received in revised form 4 May 2020; Accepted 5 May 2020
Available online 10 May 2020

surface pores upon hydration. Then, water goes into the amorphous region and preferentially hydrates this region over the crystalline structure (Gallay & Puddington, 1943; Tako, Tamaki, Teruya, & Takeda, 2014; Zobel, Young, & Rocca, 1988). The water absorption capacity of starch is dependent on the number of pores, channels, and cavities within the starch granule (Wang et al., 2016; Weirong & Huiyuan, 2002).

Porous starch is a modified starch product which is prepared to enhance the porosity of native starch, thus increasing its water absorption capacity (Wang et al., 2016; Weirong & Huiyuan, 2002). Another type of starch that exhibits high water absorption capacity is cold water swelling starch (CWSS). Many studies have reported the capability of CWSS to absorb water at low temperatures (Dries, Gomand, Goderis, & Delcour, 2014; Rajagopalan & Seib, 1992). CWSS can absorb water up to 12 times more than its weight (Majzoobi, Kaveh, Blanchard, & Farahnaky, 2015). Meanwhile, porous starch can only maximally absorb water up to 3 times more than its weight (Wang et al., 2016). Therefore, it is advantageous to use CWSS over porous starch because of its greater water absorption capacity.

Among methods to prepare CWSS, heating starch with ethanol, which is commonly termed as ethanol-treated starch (ETS), is considered to be the simplest method. It only requires ethanol as the converting reactant which can be removed from the product by dehydration, thus leaving little or no residue of this reagent in the final product (Dries et al., 2014; Zhang, Dhital, Haque, & Gidley, 2012).

Porous starch contains pores in the macropore range since its pore diameter is predominantly about 1 μm (Sujka & Jamroz, 2009, 2010). Among porous starches porous rice starch has the highest surface area (1.66 m^2/g) meanwhile porous potato starch has the lowest area (0.4 m^2/g) (Lesław Juszczak et al., 2002; Sujka & Jamroz, 2010). Therefore, porous rice starch possesses a high potential for use as a carrying agent (Sujka & Jamroz, 2010).

The capability of ETS to absorb high amount of water can be an indication that it has high porosity. As proposed by Jane, Craig, Seib, and Hoseney (1986) that the structure of native starch drastically changes after it is converted to ETS. The crystalline structure of amylopectin double helix melts and it turns to amorphous structure of amylopectin single helix. According to the free volume theory, amorphous structure provides more free space therefore allowing guest molecules to reside within it (Turnbull & Cohen, 1961). However, since the pore characterizations of ETS have not yet been conducted, the cause of high water absorption capability of ETS is still unclear. Thus, the main objective of the present study was to investigate the pore characteristics of ETS. The influence of pore characteristics on the water absorption capacity was studied. Moreover, the impact of the structural properties of ETS on the water absorption capacity was included to gain a comprehensive view of the factors affecting this property.

2. Materials and methods

2.1. Materials

Normal maize and potato starches were supplied by National Starch and Chemicals Ltd. (Bangkok, Thailand). Rice and cassava starches were provided by General Food Product Co. Ltd. and Sanguan Wongse Industries Co. Ltd. (Nakhon Ratchasima, Thailand), respectively. Analytical grade ethanol was purchased from Carlo Erba Ltd. (Val de Reuil, France).

2.2. Sample preparation

ETS was prepared by the method of Dries et al. (2014) with some modifications. Starch (15 g) from different sources (maize (M0), potato (P0), cassava (C0), and rice (R0)) was dispersed with 135 ml of ethanol (50 %v/v) in Schott bottles. It was then heated at different temperatures of 80, 90 and 100 °C (M80, M90, M100, P80, P90, P100, C80, C90, C100, R80, R90, and R100) for 30 min and cooled at room temperature for 3 h. The sediment was separated from the supernatant by vacuum filtration, washed with absolute ethanol three times and finally dried in a vacuum oven at 55 °C for 12 h. The dried sample was ground and sieved with a sieve with aperture size of 150 μm. All treatments were carried out in triplicate.

2.3. Water absorption capacity

A method described by Wang et al. (2016) was modified to determine the water absorption capacity (WAC) of samples. A sample suspension of 0.5 g (5% (w/v)) was centrifuged (CR22GIII, Hitachi, Japan) at 1500 rpm for 10 min. The sediment was carefully separated from the supernatant. The WAC was determined according to the following equation:

$$\text{WAC } [\%] = \frac{\text{the weight of sediment [g]} - \text{the initial weight of sample [g]}}{\text{the initial weight of sample [g]}} \text{ x } 100\ \% \quad (1)$$

2.4. Morphological properties

The morphological properties of the samples were observed by a Field Emission-Scanning Electron Microscope (AurigaTm-Carl Zeiss, Jena, Germany). The sample was mounted on a metal stub and coated with gold. Then, an accelerating voltage of 2 kV was used during observation.

2.5. Pore characterization by nitrogen adsorption

The pore characteristics of ETS were determined by the nitrogen gas adsorption method using BELSORP mini-II sorption isotherm apparatus (MicrotracBel Corp., Osaka, Japan). The nitrogen sorption isotherms of native starches and their corresponding ETS are shown in Fig. S1. The specific surface area (BET surface area) and pore size distribution (BJH pore size distribution) were determined from the sorption isotherm according to the IUPAC standard method (Sing et al., 1985).

2.6. The crystalline structure of ETS

The crystalline structure of ETS was assessed by the wide-angle X-ray scattering (WAXS) technique at Synchrotron Light Research Institute (SLRI), Nakhon Ratchasima, Thailand. The beamline was set according to Soontaranon and Rugmai (2012) with some modifications. A program called SAXSIT was employed to fit the crystalline peaks by the pseudo-Voigt fitting method. Then, the relative crystallinity of samples was determined by the following equation:

$$\text{Relative Crystallinity } [\%] = \frac{\text{area of crystalline peaks}}{\text{total area of diffractogram}} \text{ x } 100\% \quad (2)$$

2.7. Statistical analysis

Statistical analysis was performed using SPSS version 17.0 in which the ANOVA procedure was employed. Duncan's post-hoc test was used to verify the significant differences between the mean values ($P < 0.05$).

3. Results and discussion

3.1. The water absorption capacity of ETS

Fig. 1 displays the WAC profiles of native starches and their corresponding ETS. As the conversion temperature increased, the WAC values of all ETS samples increased proportionally independent of the

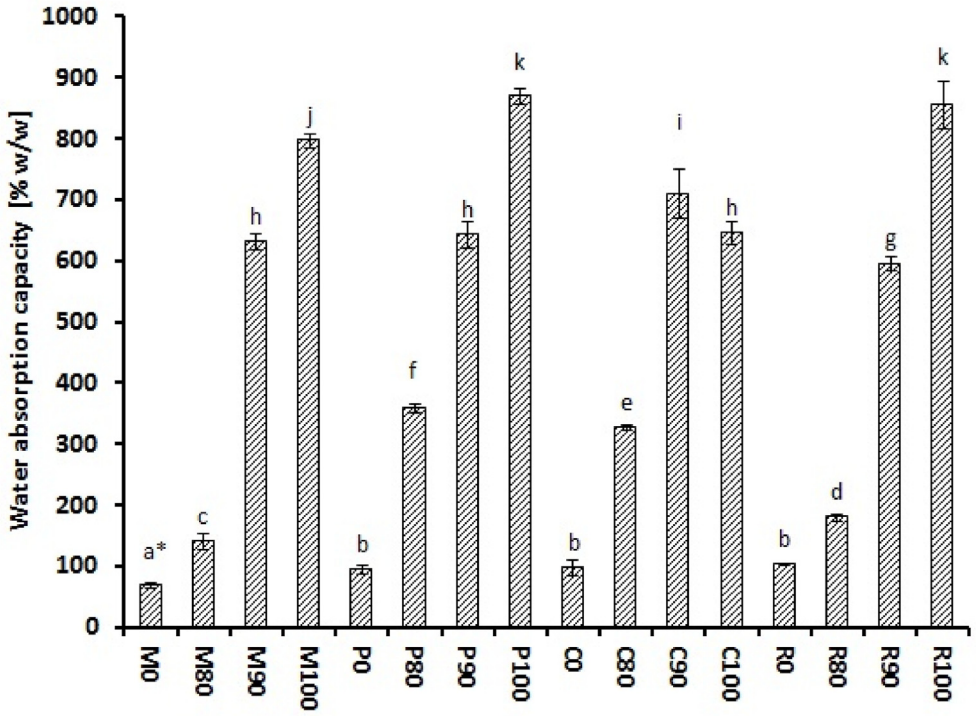

Fig. 1. The water absorption capacity of native maize (M0), potato (P0), cassava (C0), rice (R0) starch and their corresponding ethanol-treated starch (ETS) from the heating temperature of 80 °C (M80/P80/C80/R80), 90 °C (M90/P90/C90/R90) and 100 °C (M100/P100/C100/R100), respectively. Error bars represent standard deviation. * Same letters indicate that samples are not statistically different ($p > 0.05$).

origin of the native starch (Fig. 1). However, the WAC of C100 was slightly lower than that of C90. This might be because the water is difficult to penetrate into the agglomerated particles of C100 during hydration (arrows in Fig. S3, C100). The WAC values of ETS from maize, potato, cassava, and rice starches at the highest conversion temperature (100 °C) reached 796, 869, 645, and 854% w/w, respectively. These results imply that a higher heating temperature is required to obtain ETS with higher WAC. For porous starch, the highest WAC is about 300% w/w (Wang et al., 2016). The presence of physical pores has been reported to be the most important factor for the high water absorption capability of porous starch (Wang et al., 2016; Weirong & Huiyuan, 2002). For ETS, the water absorption capability might be influenced by the presence of a V-crystalline structure (Dries et al., 2014) since the V-type crystalline structure of the amylose-ethanol complex is soluble in cold water (French & Murphy, 1977).

3.2. Morphological properties of ETS

The morphological properties of native maize, potato, cassava, and rice starches and their corresponding ETS are presented in Fig. 2. The native maize starch granules exhibited polyhydric to round shapes, and some granules showed pores on their surface (Fig. 2, M0). The native potato starch granules showed oval shapes with a smooth surface (Fig. 2, P0). The native cassava starch granules displayed round shapes with some truncated and smoothed surface granules (Fig. 2, C0). The native rice starch granules showed polyhedral shapes and tended to aggregate (Fig. 2, R0) (Chen, Yu, Chen, & Li, 2006; Jivan, Yarmand, & Madadlou, 2014; L.; Juszczak, Fortuna, & Krok, 2003).

Among ETS prepared at 80 °C, the granules of P80 showed the most obvious alterations in that most granules exhibited indentation and were donut-shaped with wrinkles on their surface (Fig. 2, P80). Some granules of C80 melted and became aggregated particles with a wrinkled surface (inset of Fig. 2, C80). Also, some R80 granules were indented on their polyhedral sides (inset of Fig. 2, R80). Drastic morphological alterations were observed on the surfaces of the ETS granules from the conversion temperatures of 90 and 100 °C (Fig. 2, M90, M100, P90, P100, C90, C100, R90, and R100). The M90, M100, P90, and P100 granules showed wrinkles and fissures on the granule surfaces (insets of Fig. 2, M90, M100, P90, and P100), and some of the granules melted and stuck to each other. Moreover, M90 and M100 granules still exhibited granular forms (Fig. 2, M90 and M100). The granular structure of P90 and P100 was also still preserved (Fig. 2, P90 and P100). The capability of maize and potato starches to maintain their granular form during ETS conversion might be because they contain amylose with a high degree of polymerization (DP) (McDonagh, 2012, pp. 162–174) and amylose tie-chains (Saibene & Seetharaman, 2010). Long amylose and amylose tie-chains hold their granular form tightly preventing them from excessive disruption during heating (Cheetham & Tao, 1998; Saibene & Seetharaman, 2010). In addition, ETS contains a V-type crystalline structure which also prevents the ETS granules from collapse (Dries et al., 2014; Dries, Gomand, Delcour, & Goderis, 2016; Sarifudin, Soontaranon, Rugmai, & Tongta, 2019; Zhang et al., 2012). It is suggested that these factors work collaboratively to prevent pore collapse and preserve the ETS granule integrity (Dries et al., 2014, 2016; Sarifudin et al., 2019).

Granules of C90, C100, R90, and R100 underwent extreme morphological transformations in which the granules were destroyed, melted and formed agglomerates (Fig. 2, C90, C100, R90, and R100). The granular shapes of C100 and R100 were also not maintained; instead, debris shaped-like particles were observed. Rice and cassava starch granules are known to be easily disrupted because the role of amylose in maintaining the granules' integrity is limited due to the fact that the amylose of rice starch has low DP (Dries et al., 2016) and cassava starch lacks amylose-tie chains (Rolland-Sabaté et al., 2012).

3.3. Pore characteristics of ethanol-treated starch

The profiles of the BET surface areas of native starches and their corresponding ETS are displayed in Fig. 3. In accordance with the previous reports (Sujka & Jamroz, 2007, 2009, 2010) among the native starches, rice starch exhibited the highest value (1.07 m^2/g), followed by maize starch (0.83 m^2/g), cassava starch (0.69 m^2/g), and the lowest value was for potato starch (0.35 m^2/g).

The BET surface areas of ETS from maize and potato starches

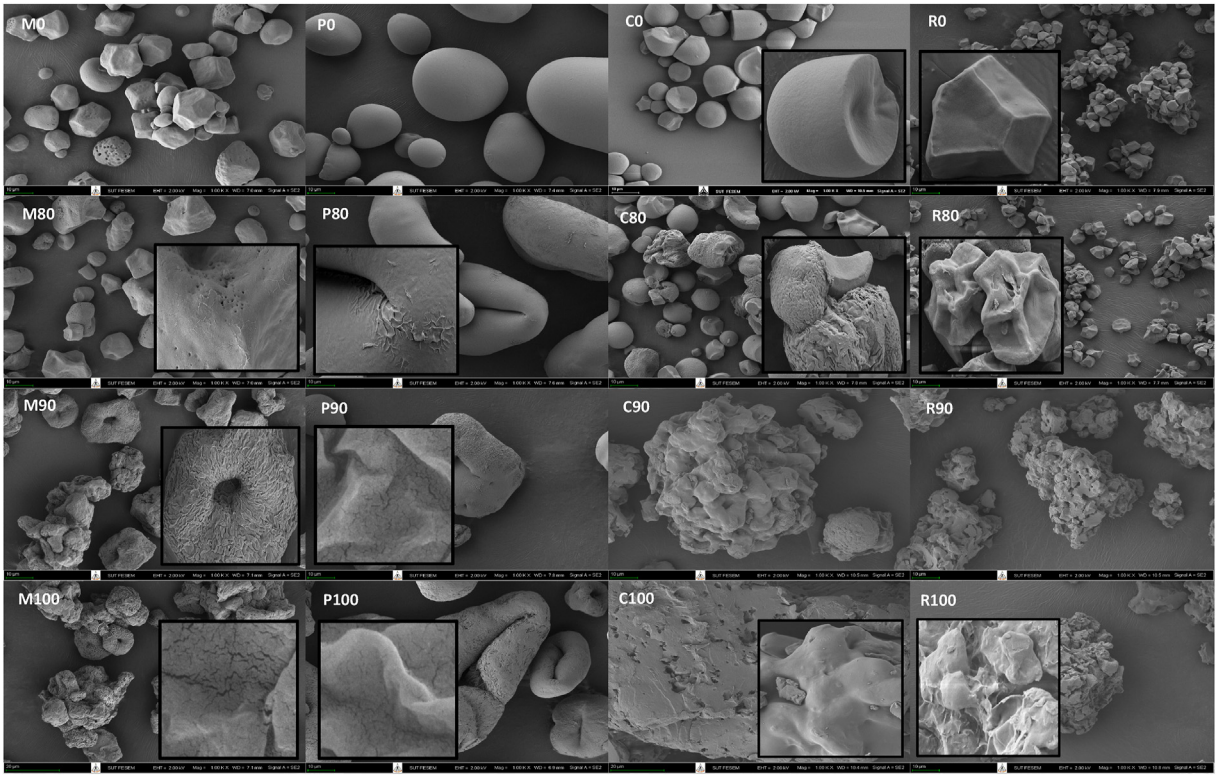

Fig. 2. Scanning electron micrograph of native maize (M0), potato (P0), cassava (C0), rice (R0) starch and their corresponding ethanol-treated starch (ETS) from the heating temperatures of 80 °C (M80/P80/C80/R80), 90 °C (M90/P90/C90/R90) and 100 °C (M100/P100/C100/R100), respectively.

increased as the temperature increased (Fig. 3). The BET surface areas of M100 and P100 reached 3.2 and 2.3 m^2/g, respectively. These results suggest that for ETS from maize and potato starches, new pores are formed during ETS conversion, resulting in the increase of the starch surface areas (Lowell et al., 2010). At the high conversion temperatures (90 and 100 °C), the ETS from maize and potato starches still showed granular forms (Fig. 2, M90, M100, P90, and P100). This result implies that the pores of ETS from maize and potato starches are located within the ETS granules. The sorption isotherms of M90, M100, P90, and P100 showed S-shapes with wider hysteresis gaps at a high partial pressure (p/po 0.6–0.99) (Fig. S1, M90, M100, P90, and P100). These hysteresis shapes are almost similar to type H3 of the IUPAC hysteresis shapes (Lowell et al., 2010; Seaton, 1991). This suggests that the pore of ETS are slit-shaped in form as indicated by the slit-shaped fissures on the ETS granule surfaces (insets of Fig. 2, M90, M100, P90, and P100). The S-shapes of the sorption isotherms indicate that the pores of ETS have characteristic of non-rigid pores (Lowell et al., 2010). Pores with non-rigid features are more susceptible to environmental conditions, i.e., temperature, pressure, and interaction potential between the vapor (adsorbate) and the pore surface (Lowell et al., 2010). Upon soaking,

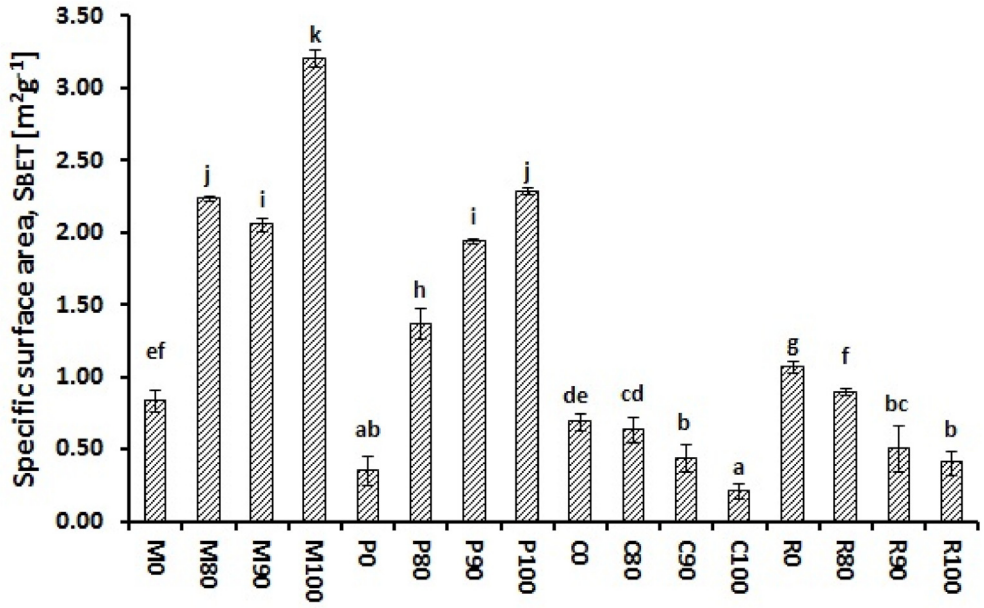

Fig. 3. The specific surface area of native maize (M0), potato (P0), cassava (C0) and rice (R0) starch and their corresponding ethanol-treated starch (ETS) from the heating temperatures of 80 °C (M80/P80/C80/R80), 90 °C (M90/P90/C90/R90) and 100 °C (M100/P100/C100/R100), respectively. * Same letters represent that samples are not statistically different ($p > 0.05$).

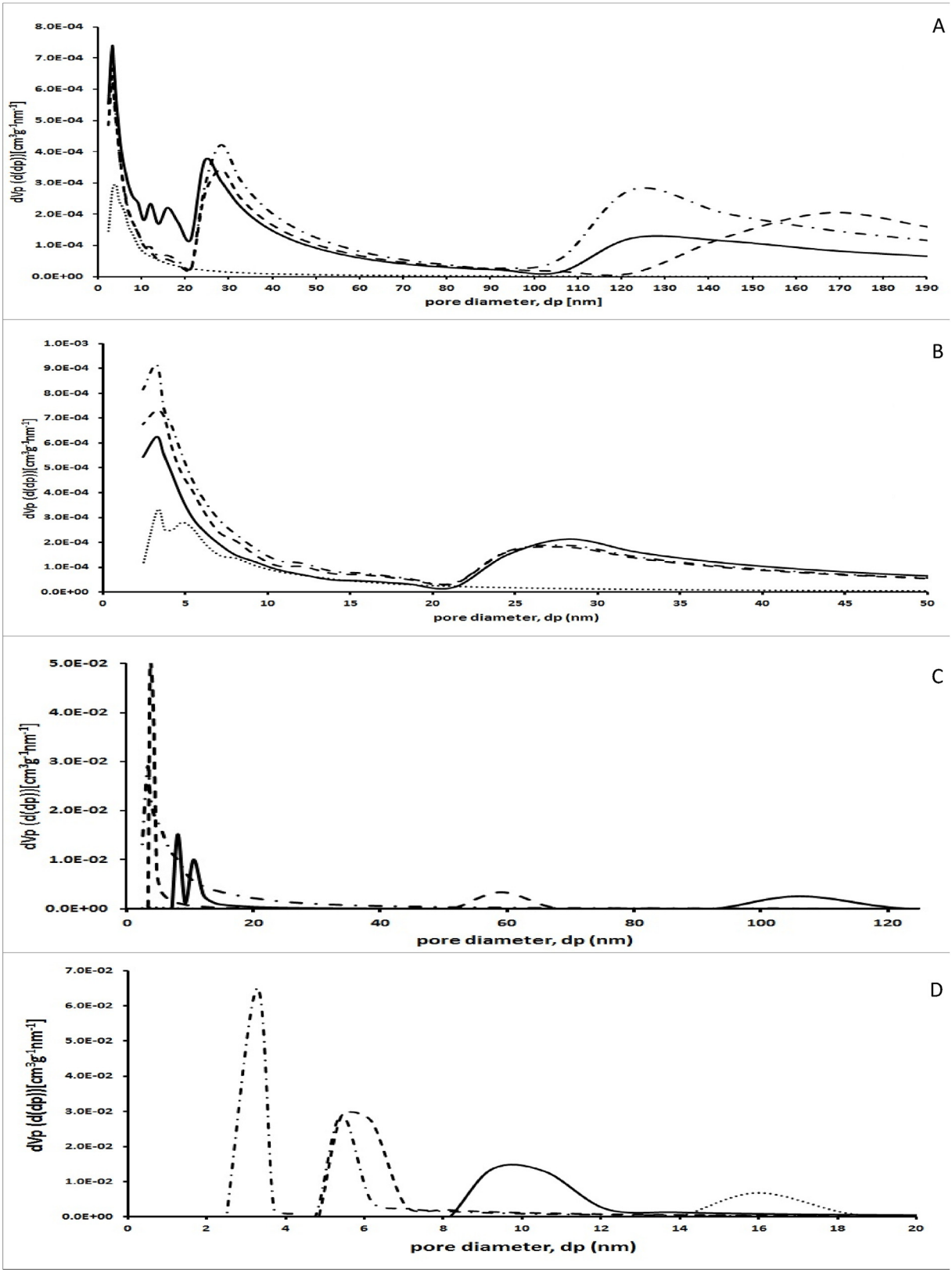

Fig. 4. Pore size distribution of native (··· ···) maize (M0) (A), potato (P0) (B), cassava (C0) (C), rice (R0) (D) starch and their corresponding ethanol-treated starch (ETS) from the heating temperatures of 80 °C (——) (M80/P80/C80/R80), 90 °C (– –) (M90/P90/C90/R90) and 100 °C (– · –) (M100/P100/C100/R100), respectively.

water molecules immediately hydrate the surface of starch granule and penetrate the starch granules through the surface pores. Then, the interactions between water and hydroxyl groups of starch components via hydrogen bonding occur, hence modifying the internal energy of the starch granules and resulting in the granule's swelling (Khankari & Grant, 1995). The impact of hydration effects is more pronounce due to starch granules contain pores with non-rigid characteristic; thus, the starch granules are easy to swell (Fig. S3, M90, M100, P90, and P100).

Meanwhile, the BET surface areas of ETS from cassava and rice starches decreased as the temperature increased (Fig. 3). The BET surface areas of C100 and R100 were 0.2 and 0.4 m^2/g, respectively. Moreover, the hysteresis gaps of C90, C100, R80, R90 and R100 isotherms at a high partial pressure have not developed (Fig. S1, C90, C100, R80, R90, and R100, respectively). These results indicates that pores which exist in native rice and cassava starches were annihilated during ETS conversion, resulting in the decrease of the granule surface areas (Fig. 3) which is confirmed by the morphological data (Fig. 2, C90, C100, R90, and R100).

The profiles of the pore size distribution of native starches and their corresponding ETS are shown in Fig. 4. Different starch sources possess different pore size distribution profiles. The native maize starch shows a broad pore size distribution in the mesopore range (2–50 nm) with major pores of 3.8 nm in size. The native potato also exhibits a bimodal pore size distribution profile in which the major pores are 3.3 and 4.8 nm. The native cassava and rice starches show a narrower pore size distribution with major pores of 3.7 and 16 nm, respectively.

The results of the pore size distribution analysis suggest that for ETS from maize starch, the new pores which were formed during the ETS conversion have a pore size distribution within the mesopore and macropore ranges (Fig. 4, A). Meanwhile, for ETS from potato starch, the new pores have a pore size distribution in the mesopore ranges (Fig. 4, B). The new pores formed during ETS conversion may have originated from granules cracking as indicated by fissures on the ETS granule surfaces (insets of Fig. 2, M90, M100, P90, and P100). The pores of ETS from cassava and rice starches are of a smaller size than those of their native starches (Fig. 4C and D) which could be due to pore collapse as indicated by the low surface areas (Fig. 3) and morphological data of both starches after ETS conversion (Fig. 2, C90, C100, R90, and R100).

3.4. The crystalline structure of ETS

The WAXS patterns of native starches and their corresponding ETS are shown in Fig. S2, and their crystallinity profiles are displayed in Fig. 5. The peaks of V-type crystalline structure of all ETS samples, which were identified at 2θ of 7.8°, 13.6°, and 20.9° (Le Bail, Bizot, Pontoire, & Buleon, 1995) emerged at 90 and 100 °C. However, the V-type crystalline structure of ETS from cassava starch appeared at a lower temperature (80 °C) (Figs. S2 and C) which might be because the amyloses of cassava starch are in free form (Rolland-Sabaté et al., 2012). Therefore, it is easier to form a V-type crystalline structure at a low temperature (80 °C). M90 and M100 showed doublet peaks at 2θ of 19.8° and 20.9° which were probably the result of a mixture of two V-type crystalline structures, namely Vh and Va, respectively (Le Bail et al., 1995). ETS contains a high proportion of V-type crystalline structure of the amylose-ethanol complex (Dries et al., 2014; Zhang et al., 2012) which is known to be water soluble (French & Murphy, 1977).

When the ETS conversion temperature increased, the native crystallinity decreased drastically, and the V-type crystallinity increased proportionally (Fig. 5). During ETS conversion, the crystalline region was destroyed, consequently increasing the amorphous proportion (Fig. 5). The amorphous structure is known to have more voids within its structure (Jenkins & Donald, 1998); therefore, water penetrates and hydrates an amorphous structure easily than a crystalline structure (Gallay & Puddington, 1943; Tako et al., 2014; Zobel et al., 1988).

Two mechanisms for the water absorption of ETS are proposed. For granular ETS from maize and potato starches, when the ETS granules are in contact with water, water penetrates the ETS granules via fissures on the surface (insets of Fig. 2, M90, M100, P90, and P100). Then, water passes through the new pores which are formed during the ETS conversion (Fig. 4A and B). The pores of granular ETS from maize and potato starches with mesopore and macropore sizes allow water to penetrate the ETS granules. Water preferentially penetrates and hydrates the amorphous structure and also melts the V-type crystalline structure. Since ETS granules contain non-rigid pores (downside insets of Fig. S1), (Lowell et al., 2010; Sing et al., 1985) the ETS granules are easy to swell by water. Finally, water is held within the ETS granules of maize and potato starches (arrows in Fig. S3, M80, M90, M100, P80, P90, and P100). Meanwhile, upon hydration of the non-granular ETS from cassava and rice starches, water is in direct contact with the amorphous regions at the outer surfaces of ETS particles (Fig. 2, C90, C100, R90, and R100). Then, the starch components in amorphous structures move slightly and become entangled with the neighboring starch components forming a three-dimensional network of a typical amylose-amylopectin-water gel structure which is commonly found in the gel system of fully gelatinized starch (Kawabata, Akuzawa, Ishii, Yazaki, & Otsubo, 1996). Thus, for non-granular ETS from cassava and rice starches, water is entrapped within the three-dimensional structure of starch components upon water absorption (arrows in Fig. S3, C90, C100, R90, and R100).

Based on the results, ETS is potential for some industrial applications. The ETS that show high surface area with intact granular shapes, such as M90, M100, P90, and P100, are prospective for encapsulating agent. These ETS exhibit high porosity that allows active ingredients to penetrate into their granules (arrows in Fig. S3, M90, M100, P90, and P100). Moreover, these ETS might be more efficient for encapsulating material than porous starch. This is because these ETS show higher

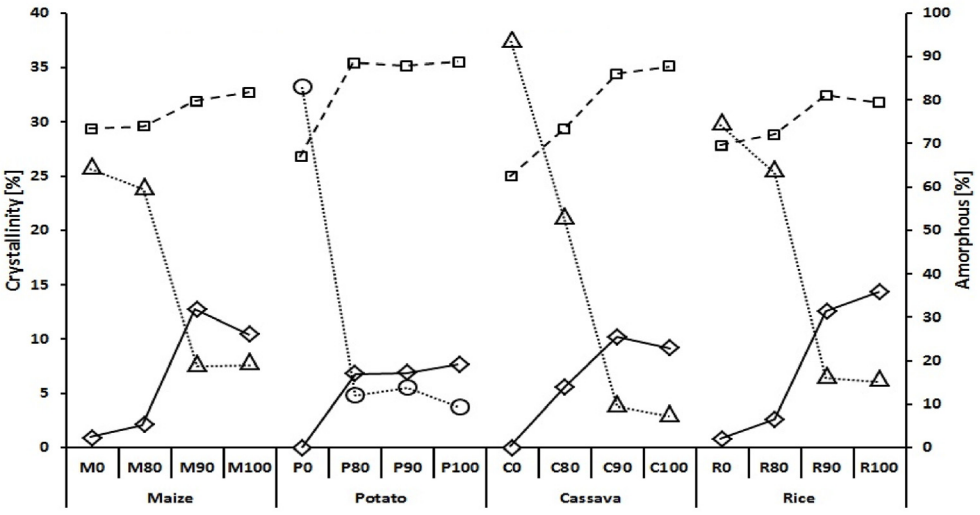

Fig. 5. Crystallinity profile of native maize (M0), potato (P0), cassava (C0) and rice (R0) starch and their corresponding ethanol-treated starch (ETS) from the heating temperatures of 80 °C (M80/P80/C80/R80), 90 °C (M90/P90/C90/R90) and 100 °C (M100/P100/C100/R100) including A-type crystalline (Δ), B-type crystalline (o) and V-type crystalline (◊), and amorphous (□) structures, respectively.

WAC (600–900% w/w) (Fig. 1) than porous starch (300% w/w) (Wang et al., 2016). The ETS that show high WAC but without granular forms, such as C90, C100, R90, and R100, can be applicable for ingredients of instantaneous products (Eastman, 1987) and sustained-release medicinal tablet (Sarifudin, Soontaranon, Peerapattana, & Tongta, 2020). Water is entrapped within a matrix formed by the ETS particles entanglement (arrows in Fig. S3, C90, C100, R90, and R100).

4. Conclusions

The pore characteristics and structural properties influence the water absorption capacity of ETS. Pores of ETS are characteristically non-rigid and slit-shaped pores. During ETS conversion, the new pores are formed for ETS from maize and potato starches; meanwhile, the pores are annihilated for ETS from cassava and rice starches. ETS produced at higher conversion temperatures contains a higher percentage of V-type crystalline and amorphous structures. Upon water absorption, water penetrates the ETS granules via fissures on the surface; then, it passes through the new pores to enter the ETS granules, hydrate the amorphous region and melt the V-type crystalline structure. For granular ETS from maize and potato starches, water is kept within the ETS granules upon water absorption. For non-granular ETS from cassava and rice starches, water hydrates the amorphous structure of the ETS particles and melts the V-type crystalline structure. Then, the water is entrapped within the three-dimensional assembly of starch components upon hydration.

CRediT authorship contribution statement

Achmat Sarifudin: Conceptualization, Methodology, Investigation, Data curation, Writing - original draft. **Thewika Keeratiburana:** Validation, Data curation. **Siriwat Soontaranon:** Validation, Formal analysis. **Chaiyot Tangsathitkulchai:** Conceptualization, Supervision. **Sunanta Tongta:** Conceptualization, Project administration, Methodology, Supervision, Writing - review & editing.

Declaration of competing interest

The authors confirm that there are no known conflicts of interest associated with this publication.

Acknowledgments

The authors are grateful for the financial support of the 2015 Suranaree University of Technology (SUT)-PhD scholarship program for ASEAN countries.

Appendix A. Supplementary data

Supplementary data to this article can be found online at https://doi.org/10.1016/j.lwt.2020.109555.

References

Cheetham, N. W. H., & Tao, L. (1998). Variation in crystalline type with amylose content in maize starch granules: An X-ray powder diffraction study. *Carbohydrate Polymers, 36*(4), 277–284. https://doi.org/10.1016/S0144-8617(98)00007-1.

Chen, P., Yu, L., Chen, L., & Li, X. (2006). Morphology and microstructure of maize starches with different amylose/amylopectin content. *Starch Staerke, 58*(12), 611–615. https://doi.org/10.1002/star.200500529.

Dries, D. M., Gomand, S. V., Delcour, J. A., & Goderis, B. (2016). V-type crystal formation in starch by aqueous ethanol treatment: The effect of amylose degree of polymerization. *Food Hydrocolloids, 61*, 649–661. https://doi.org/10.1016/j.foodhyd.2016.06.026.

Dries, D. M., Gomand, S. V., Goderis, B., & Delcour, J. A. (2014). Structural and thermal transitions during the conversion from native to granular cold-water swelling maize starch. *Carbohydrate Polymers, 114*, 196–205. https://doi.org/10.1016/j.carbpol.2014.07.066.

Eastman, J. E. (1987). *USA patent No. 4.634.596. USPTO*.

Fannon, J. E., Hauber, R. J., & Bemiller, J. N. (1992). Surface pores of starch granules. *Cereal Chemistry, 69*, 284–288.

French, A. D., & Murphy, V. G. (1977). Computer modeling in the study of starch. *Cereal Foods World, 22*(2), 61–70.

Gallay, W., & Puddington, I. E. (1943). The hydration of starch below the gelatinization temperature. *Canadian Journal of Research, 21b*(9), 179–185. https://doi.org/10.1139/cjr43b-024.

Hall, D. M., & Sayre, J. G. (1970). A scanning electron-microscope study of starches. *Textile Research Journal, 40*(3), 256–266. https://doi.org/10.1177/004051757004000309.

Huber, K. C., & BeMiller, J. N. (1997). Visualization of channels and cavities of corn and sorghum starch granules. *Cereal Chemistry, 74*(5), 537–541. https://doi.org/10.1094/CCHEM.1997.74.5.537.

Jane, J., Craig, S. A. S., Seib, P. A., & Hoseney, R. C. (1986). Characterization of granular cold water-soluble starch. *Starch Staerke, 38*, 258–263.

Jenkins, P. J., & Donald, A. M. (1998). Gelatinisation of starch: A combined SAXS/WAXS/DSC and SANS study. *Carbohydrate Research, 308*(1), 133–147. https://doi.org/10.1016/S0008-6215(98)00079-2.

Jivan, M. J., Yarmand, M., & Madadlou, A. (2014). Preparation of cold water-soluble potato starch and its characterization. *Journal of Food Science & Technology, 51*(3), 601–605. https://doi.org/10.1007/s13197-013-1200-yhttps://search.crossref.org/?q=Preparation+of+cold+water-soluble+potato+starch+and+its+characterization.+Journal+of+Food+Science+%26+Technology.

Juszczak, L., Fortuna, T., & Krok, F. (2003). Non-contact atomic force microscopy of starch granules surface. Part I. Potato and tapioca starches. *Starch Staerke, 55*, 1–7. https://doi.org/10.1002/star.200390012.

Juszczak, L., Fortuna, T., & Wodnicka, K. (2002). Characteristics of cereal starch granules surface using nitrogen adsorption. *Journal of Food Engineering, 54*(2), 103–110. https://doi.org/10.1016/S0260-8774(01)00190-X.

Karathanos, V. T., & Saravacos, G. D. (1993). Porosity and pore size distribution of starch materials. *Journal of Food Engineering, 18*(3), 259–280. https://doi.org/10.1016/0260-8774(93)90090-7.

Kawabata, A., Akuzawa, S., Ishii, Y., Yazaki, T., & Otsubo, Y. (1996). Sol-gel transition and elasticity of starch. *Bioscience Biotechnology and Biochemistry, 60*(4), 567–570. https://doi.org/10.1271/bbb.60.567.

Khankari, R. K., & Grant, D. J. W. (1995). Pharmaceutical hydrates. *Thermochimica Acta, 248*, 61–79. https://doi.org/10.1016/0040-6031(94)01952-D.

Le Bail, P., Bizot, H., Pontoire, B., & Buleon, A. (1995). Polymorphic transitions of amylose-ethanol crystalline complexes induced by moisture exchanges. *Starch Staerke, 47*(6), 229–232. https://doi.org/10.1002/star.19950470608.

Lowell, S., Shields, J. E., Thomas, M. A., & Thommes, M. (2010). *Characterization of porous solids and powders: Surface area, pore size and density*. Kluwer Academic Publishers, Springer.

Majzoobi, M., Kaveh, Z., Blanchard, C. L., & Farahnaky, A. (2015). Physical properties of pregelatinized and granular cold water swelling maize starches in presence of acetic acid. *Food Hydrocolloids, 51*, 375–382. https://doi.org/10.1016/j.foodhyd.2015.06.002.

McDonagh, P. (2012). *7 - native, modified and clean label starches in foods and beverages Natural Food Additives, Ingredients and Flavourings*. Woodhead Publishing.

Najafi, S. H. M., Baghaie, M., & Ashori, A. (2016). Preparation and characterization of acetylated starch nanoparticles as drug carrier: Ciprofloxacin as a model. *International Journal of Biological Macromolecules, 87*, 48–54. https://doi.org/10.1016/j.ijbiomac.2016.02.030.

Rajagopalan, S., & Seib, P. A. (1992). Properties of granular cold-water-soluble starches prepared at atmospheric pressure. *Journal of Cereal Science, 16*(1), 29–40. https://doi.org/10.1016/S0733-5210(09)80077-5.

Rolland-Sabaté, A., Sánchez, T., Buléon, A., Colonna, P., Jaillais, B., Ceballos, H., et al. (2012). Structural characterization of novel cassava starches with low and high-amylose contents in comparison with other commercial sources. *Food Hydrocolloids, 27*(1), 161–174. https://doi.org/10.1016/j.foodhyd.2011.07.008.

Saibene, D., & Seetharaman, K. (2010). Amylose involvement in the amylopectin clusters of potato starch granules. *Carbohydrate Polymers, 82*(2), 376–383. https://doi.org/10.1016/j.carbpol.2010.04.070.

Sarifudin, A., Soontaranon, S., Peerapattana, J., & Tongta, S. (2020). Mechanical strength, structural and hydration properties of ethanol-treated starch tablets and their impact on the release of active ingredients. *International Journal of Biological Macromolecules, 149*, 541–551. https://doi.org/10.1016/j.ijbiomac.2020.01.286.

Sarifudin, A., Soontaranon, S., Rugmai, S., & Tongta, S. (2019). Structural transformations at different organizational levels of ethanol-treated starch during heating. *International Journal of Biological Macromolecules, 132*, 1131–1139. https://doi.org/10.1016/j.ijbiomac.2019.04.025.

Seaton, N. A. (1991). Determination of the connectivity of porous solids from nitrogen sorption measurements. *Chemical Engineering Science, 46*(8), 1895–1909. https://doi.org/10.1016/0009-2509(91)80151-N.

Sing, K. S. W., Everett, D. H., Haul, R. A. W., Moscou, L., Pierotti, R. A., Rouquerol, J., et al. (1985). Reporting physisorption data for gas/solid systems with special reference to the determination of surface area and porosity (Recommendations 1984). *Pure and Applied Chemistry, 57*(4), 603–619. https://doi.org/10.1002/9783527610044.hetcat0065.

Soontaranon, S., & Rugmai, S. (2012). Small angle X-ray scattering at siam photon laboratory. *Chinese Journal of Physics, 50*(2), 204–210.

Sujka, M., & Jamroz, J. (2007). Starch granule porosity and its changes by means of amylolysis. *International Agrophysics, 21*, 107–113.

Sujka, M., & Jamroz, J. (2009). α-Amylolysis of native potato and corn starches – SEM, AFM, nitrogen and iodine sorption investigations. *LWT Food Science and Technology, 42*(7), 1219–1224. https://doi.org/10.1016/j.lwt.2009.01.016.

Sujka, M., & Jamroz, J. (2010). Characteristics of pores in native and hydrolyzed starch granules. *Starch Staerke, 62*(5), 229–235. https://doi.org/10.1002/star.200900226.

Tako, M., Tamaki, Y., Teruya, T., & Takeda, Y. (2014). The principles of starch gelatinization and retrogradation. *Food and Nutrition Sciences, 5*(3), 280–291. https://doi.org/10.4236/fns.2014.53035.

Turnbull, D., & Cohen, M. H. (1961). Free-volume model of the amorphous phase: Glass transition. *The Journal of Chemical Physics, 34*(1), 120–125. https://doi.org/10.1063/1.1731549.

Wang, H., Lv, J., Jiang, S., Niu, B., Pang, M., & Jiang, S. (2016). Preparation and characterization of porous corn starch and its adsorption toward grape seed proanthocyanidins. *Starch Staerke, 68*(11–12), 1254–1263. https://doi.org/10.1002/star.201600009.

Weirong, Y., & Huiyuan, Y. (2002). Adsorbent characteristics of porous starch. *Starch Staerke, 54*(6), 260–263. https://doi.org/10.1002/1521-379X(200206)54:6<260::AID-STAR260>3.0.CO;2-Z.

Zhang, B., Dhital, S., Haque, E., & Gidley, M. J. (2012). Preparation and characterization of gelatinized granular starches from aqueous ethanol treatments. *Carbohydrate Polymers, 90*(4), 1587–1594. https://doi.org/10.1016/j.carbpol.2012.07.035.

Zobel, H. F., Young, S. N., & Rocca, L. A. (1988). Starch gelatinization: An X-ray diffraction study. *Cereal Chemistry, 65*(6), 443–446.